Accepted Manuscript

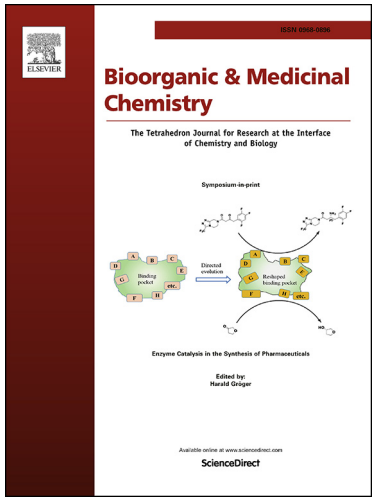

Syntheses and evaluation of a homologous series of aza-vesamicol as improved radioiodine-labeled probes for sigma-1 receptor imaging

Kazuma Ogawa, Ryohei Masuda, Kenji Mishiro, Mengfei Wang, Takashi Kozaka, Kazuhiro Shiba, Seigo Kinuya, Akira Odani

PII: S0968-0896(18)31998-9
DOI: https://doi.org/10.1016/j.bmc.2019.03.054
Reference: BMC 14846

To appear in: *Bioorganic & Medicinal Chemistry*

Received Date: 26 November 2018
Revised Date: 27 March 2019
Accepted Date: 29 March 2019

Please cite this article as: Ogawa, K., Masuda, R., Mishiro, K., Wang, M., Kozaka, T., Shiba, K., Kinuya, S., Odani, A., Syntheses and evaluation of a homologous series of aza-vesamicol as improved radioiodine-labeled probes for sigma-1 receptor imaging, *Bioorganic & Medicinal Chemistry* (2019), doi: https://doi.org/10.1016/j.bmc.2019.03.054

Syntheses and evaluation of a homologous series of aza-vesamicol as improved radioiodine-labeled probes for sigma-1 receptor imaging

Kazuma Ogawa[a,b*], Ryohei Masuda[b], Kenji Mishiro[a], Mengfei Wang[b], Takashi Kozaka[c], Kazuhiro Shiba[c], Seigo Kinuya[b], Akira Odani[b]

[a]*Institute for Frontier Science Initiative, Kanazawa University, Kakuma-machi, Kanazawa, Ishikawa 920-1192, Japan;*

[b]*Graduate School of Pharmaceutical Sciences, Kanazawa University, Kakuma-machi, Kanazawa, Ishikawa 920-1192, Japan;*

[c]*Advanced Science Research Centre, Kanazawa University, Takara-machi, Kanazawa, Ishikawa 920-8640, Japan;*

***Corresponding Author:**

Kazuma Ogawa Telephone: 81-76-234-4460; Fax: 81-76-234-4459

E-mail: kogawa@p.kanazawa-u.ac.jp

Running Title: sigma-1 receptor imaging probe

Conflict of interest: The authors have declared that no conflict of interest.

Abstract

Sigma-1 receptor imaging probes for determining the expression levels are desirable for diagnoses of various diseases and companion diagnoses of therapeutic agents targeting the sigma-1 receptor. In this study, we aimed to develop probes with higher affinity for the sigma-1 receptor. For this purpose, we synthesized and evaluated compounds, namely, vesamicol derivatives, in which alkyl chains of varying chain length were introduced between a piperazine ring and a benzene ring. The binding affinity of the vesamicol derivatives for the sigma-1 receptor tended to increase depending on the length of the alkyl chain between the benzene ring and the piperazine ring. The sigma-1 receptor of 2-(4-(3-phenylpropyl)piperazin-1-yl)cyclohexan-1-ol (**5**) (K_i = 5.8 nM) exhibited the highest binding affinity; therefore, we introduced radioiodine into the benzene ring in **5**. The radioiodine labeled probe [^{125}I]2-(4-(3-(4-iodophenyl)propyl)piperazin-1-yl)cyclohexan-1-ol ([^{125}I]**10**) showed high accumulation in the sigma-1 receptor expressing DU-145 cells both *in vitro* and *in vivo*. Co-injection of [^{125}I]**10** with an excess level of a sigma

receptor ligand, haloperidol, resulted in a significant decrease in the tumor accumulation *in vitro* and *in vivo*, indicating sigma receptor-mediated tumor uptake. These results provide useful information for developing sigma-1 receptor imaging probes.

Key Words: Sigma-1 receptor; Imaging; Probe; Radiolabel

1. Introduction

Sigma receptors were originally regarded as a new subtype of the opioid receptors by Martin et al. (1976).[1] These receptors were subsequently reclassified as original receptors with at least two subtypes, sigma-1 and sigma-2.[2] The sigma-1 receptor was cloned over 20 years ago,[3] and the sigma-2 receptor was cloned recently.[4] The molecular size of the sigma-1 receptor is 25.3 kDa, comprising 223 amino acids; this receptor is located primarily on the endoplasmic reticulum (ER) membrane of the cell. The sigma-1 receptor works to maintain cellular homeostasis as a molecular chaperone[5, 6] and is related to functions of the central nervous system, including signal transduction, memory, recognition, and emotion. Therefore, the expression level of the sigma-1 receptor is involved in neurodegenerative diseases, such as Alzheimer's disease, Parkinson's disease, and amyotrophic lateral sclerosis (ALS).[7-9] Furthermore, it has been reported that the sigma-1 receptor is highly expressed in various cancer cells.[10] This receptor may control the electrical plasticity of cancer cells by driving ion channels to enhance their function, providing a suitable environment for cancer cells.[11] Therefore, sigma-1 receptor targeting

agents, including sigma-1 receptor agonists for neurodegenerative diseases and sigma-1 receptor antagonists for cancer therapy, may have potential for use in therapy for these diseases.[12, 13] With this background, the determination of sigma-1 receptor expression levels *in vivo* should be beneficial for the diagnosis and therapeutics treatment of diseases related to the sigma-1 receptor and for the development of drugs targeting the sigma-1 receptor.[14] The nuclear medicine technique based on radiolabeled probes is currently the only modality that can determine receptor expression levels *in vivo*. Therefore, excellent sigma-1 imaging probes are desirable for determining expression levels and, thus, may be useful for companion diagnoses of therapeutic agents targeting this receptor.[15]

We previously developed radiolabeled compounds targeting the sigma-1 receptor based on the vesamicol structure (Figure. 1a) as a lead compound.[16-21] In these studies, 2-[4-(4-iodophenyl)piperidino] cyclohexanol (*p*IV, Figure. 1b) with an iodine at the *para* position of the benzene ring in the vesamicol structure was shown to have a higher binding affinity for the sigma-1 receptor compared with vesamicol and compounds with an iodine at the *meta* or *ortho* position. Moreover, most reported

sigma-1 receptor ligands have a cationic amine and an aromatic ring.[22] In a recent X-ray crystallography study, it was demonstrated that the sigma-1 receptor and its ligands bind via electrostatic interaction between 172Glu in the sigma-1 receptor and a cationic amine in the sigma-1 receptor ligands.[23] Additionally, it has been reported that the distance between the cationic amine and hydrophobic sites influences the affinity for the sigma-1 receptor.[22]

In the structure of *p*IV, the piperidine ring and the iodobenzene sites may correspond to the cationic amine and hydrophobic sites, respectively. Thus, we hypothesized that the distance between the piperidine ring and the iodobenzene may affect the affinity for the sigma-1 receptor. To develop probes with a higher affinity for the sigma-1 receptor, we synthesized and evaluated compounds in which the piperidine ring was transformed to a piperazine ring for easy synthesis and alkyl chains of varying chain lengths were introduced between the piperazine ring and the benzene ring (Scheme 1). From among the synthesized vesamicol derivatives, we selected a compound with high affinity for the sigma-1 receptor. The compound was radiolabeled by introducing radioiodine at the *para* position on the benzene

ring because *para* was discovered to be the optimal position for enhancing the affinity of the sigma-1 receptor in vesamicol analogs. The radiolabeled compound was evaluated *in vitro* and *in vivo*. Although we are interested in developing ^{123}I ($t_{1/2}$ = 12.3 h) labeled imaging probes for single photon emission computed tomography (SPECT), ^{125}I ($t_{1/2}$ = 59.4 d) was used in this study as an alternative radionuclide because of its long half-life.

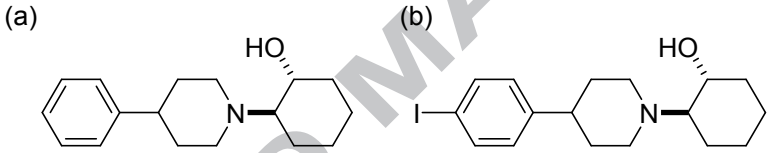

Figure 1. Structures of (a) vesamicol and (b) *p*IV.

2. Materials and methods

2.1. General

Proton nuclear magnetic resonance (^{1}H-NMR) spectra were obtained with JEOL JNM-ECS400 (JEOL Ltd, Tokyo, Japan) for 400 MHz and JNM-ECS600 (JEOL Ltd) for 600 MHz. Data for ^{1}H NMR are reported as follows: chemical shift (δ ppm), multiplicity (s = singlet, d = doublet, t = triplet, q = quartet, qt = quintet, m = multiplet), coupling

constant (Hz), and integration. Direct analysis in real time mass spectra (DART-MS) and electrospray ionization mass spectra (ESI-MS) were obtained with JEOL JMS-T100TD (JEOL Ltd). Optical rotations were measured by a model SEPA-300 high-sensitive polarimeter (HORIBA, Kyoto, Japan). [^{3}H]1,3-*o*-Di-tolylguanidine ([^{3}H]DTG) (1.1 TBq /mmol), [^{3}H]pentazocine (1.0 TBq/mmol), and [^{125}I]Sodium iodide (644 GBq/mg) were purchased from PerkinElmer (Waltham, MA, USA). TLC analyses were performed with silica plates (Art 5553, Merck, Darmstadt, Germany). SA4503 was kindly supplied by M's Science (Kobe, Japan). DTG, (+)-pentazocine, and haloperidol were purchased from Sigma-Aldrich (St. Louis, MO, USA). Other reagents were of reagent grade and used as received.

2.1. Synthesis of compounds

Synthetic scheme is shown in Schemes 1 and 2.

*2.1.1. trans-2-(4-Phenylpiperazin-1-yl)cyclohexan-1-ol (rac-**1**)*

Phenylpiperazine (1.0 g, 6.2 mmol) and cyclohexene oxide (1.2 g, 12.3 mmol) in 3.5 mL of ethanol were refluxed for 22 h. After cooling,

precipitates were washed with hexane to afford *rac*-**1** (1.5 g, 92%) as a colorless powder.

^{1}H NMR ($CDCl_3$): δ 1.24 (4H, m), 1.50-2.00 (3H, m), 2.10-2.45 (2H, m), 2.59 (2H, m), 2.89 (2H, m), 3.20 (4H, m), 3.41 (1H, m), 3.97 (1H, m), 6.86-6.94 (3H, m), 7.27 (2H, m).

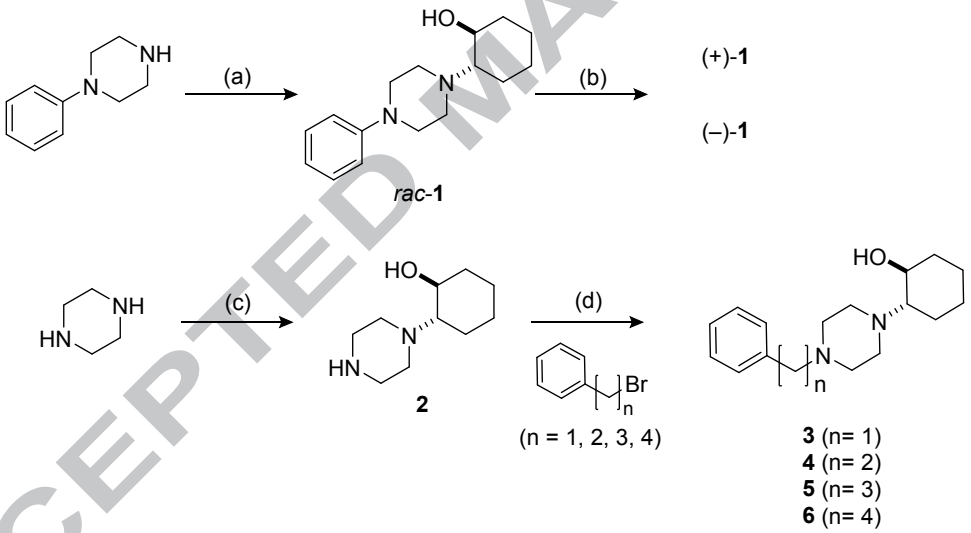

Scheme 1. Syntheses of compounds (+)-**1**, (–)-**1**, and **3**–**6**.
(a) cyclohexene oxide, ethanol; (b) di-*p*-toluoyl-D-tartaric acid, acetone; di-*p*-toluoyl-L-tartaric acid, acetone; (c) cyclohexene oxide, H_2O; (d) K_2CO_3, acetonitrile.

*2.1.2. (+)-trans-2-(4-phenylpiperazin-1-yl)cyclohexan-1-ol [(+)-(**1**)]*

(+)-Di-*p*-toluoyl-D-tartaric acid (700 mg, 5.4 mmol) was dissolved in 10 mL of acetone, and then **1** (433 mg, 1.7 mmol) in 10 mL of acetone was added dropwise to the solution at room temperature. A precipitate was collected by filtration and the filtrate was used for preparation of (–)-enantiomer of **1**. The precipitate was dissolved in 2 M aqueous NaOH solution and the solution was extracted using dichloromethane. The organic phase was dried over sodium sulfate. After the dichloromethane was removed *in vacuo*, (+)-**1** (162 mg, 75%) was obtained as a colorless powder.

^{1}H NMR (400 MHz, $CDCl_3$): δ 1.15–1.39 (m, 4H), 1.68–1.95 (m, 3H), 2.10–2.20 (m, 1H), 2.21–2.35 (m, 1H), 2.53–2.65 (m, 2H), 2.83–2.95 (m, 2H), 3.10–3.38 (m, 4H), 3.35–3.48 (m, 1H), 3.88–4.20 (m, 1H), 6.87 (t, J = 7.3 Hz, 1H), 6.93 (d, J = 8.2 Hz, 2H, m), 7.27 (dd, J = 8.7, 7.3 Hz, 2H).

HRMS (DART) m/z calcd for $C_{16}H_{25}N_2O$ $(M+H)^+$, 261.1967; found 261.1969.

Specific rotation: $[\alpha]_D^{22}$ = +16.5º (c = 0.14, methanol).

*2.1.3. (–)-trans-2-(4-phenylpiperazin-1-yl)cyclohexan-1-ol [(–)-(**1**)]*

The solvent in the filtrate was removed *in vacuo*, and the residue was dissolved in 2 M aqueous NaOH solution. The solution was extracted using dichloromethane. The organic phase was dried over sodium sulfate. The organic phase was concentrated *in vacuo* to afford a colorless solid. (–)-(**1**) was prepared by the same procedure as (+)-**1** using the residual solid (433 mg, 1.7 mmol) and (−)-di-*p*-toluoyl-L-tartaric acid (700 mg, 5.4 mmol). (–)-(**1**) (210 mg) was obtained as a colorless powder.

^{1}H NMR (400 MHz, $CDCl_3$): δ 1.15–1.39 (m, 4H), 1.68–1.95 (m, 3H), 2.10–2.20 (m, 1H), 2.21–2.35 (m, 1H), 2.53–2.65 (m, 2H), 2.83–2.95 (m, 2H), 3.10–3.38 (m, 4H), 3.35–3.48 (m, 1H), 3.70–4.15 (m, 1H), 6.87 (t, J = 7.3 Hz, 1H), 6.93 (d, J = 8.2 Hz, 2H, m), 7.27 (dd, J = 8.7, 7.3 Hz, 2H).

HRMS (DART) m/z calcd for $C_{16}H_{25}N_2O$ $(M+H)^+$, 261.1967; found 261.1969.

Specific rotation: $[\alpha]_D^{22}$ = −15.0º (c = 0.14, methanol).

*2.1.4. trans-2-(Piperazin-1-yl)cyclohexan-1-ol (**2**)*

Piperazine (851 mg, 9.9 mmol) was dissolved in 100 mL of water, and then cyclohexene oxide (970 mg, 9.9 mmol) in 100 mL of water was

added dropwise to the solution. After stirring at room temperature for 15 h, the solvent was removed *in vacuo*. The residue was purified by chromatography on silica gel using chloroform-methanol (5:1) as the eluent to obtain compound **2** (521 mg, 28%) as a colorless powder.

^{1}H NMR ($CDCl_3$): δ 1.10–1.42 (m, 4H), 1.62–1.90 (m, 3H), 2.05–2.22 (m, 2H), 2.33–2.45 (m, 2H), 2.65–2.78 (m, 2H), 2.80–2.98 (m, 4H), 3.30–3.42 (m, 1H), 3.63–3.76 (m, 1H).

*2.1.5. trans-2-(4-Benzylpiperazin-1-yl)cyclohexan-1-ol (**3**)*

Compound **2** (368 mg, 2.0 mmol) and benzyl bromide (342 mg, 2.0 mmol) were dissolved in 20 mL of acetonitrile and then potassium carbonate (276 mg, 2.0 mmol) was added to the solution. After reflux for 1 h, potassium carbonate was removed by filtration. The solvent was removed *in vacuo*. The residue was purified by chromatography on silica gel using chloroform-methanol (19:1) as the eluent to obtain compound **3** (421 mg, 77%) as a colorless powder.

^{1}H NMR (400 MHz, $CDCl_3$): δ 1.10–1.30 (4H, m), 1.65-1.85 (m, 3H), 2.05–2.15 (m, 1H), 2.15-2.23 (m, 1H), 2.25–2.65 (m, 6H), 2.68–2.80, (m,

2H), 3.30–3.39 (m, 1H), 3.51 (s, 2H), 3.95–4.05 (m, 1H), 7.25-7.30 (5H, m).

HRMS (DART) m/z calcd for $C_{17}H_{27}N_2O$ $(M+H)^+$, 275.2123; found 275.2132.

*2.1.6. trans-2-(4-Phenethylpiperazin-1-yl)cyclohexan-1-ol (**4**)*

Compound **2** (1.7 g, 9.3 mmol) and 2-phenethyl bromide (1.7 g, 9.3 mmol) were dissolved in 93 mL of acetonitrile and then potassium carbonate (1.2 g, 9.3 mmol) was added to the solution. After reflux for 1 h, potassium carbonate was removed by filtration. The solvent was removed *in vacuo*. The residue was purified by chromatography on silica gel using chloroform-methanol (20:1) as the eluent to obtain compound **4** (1.8 g, 70%) as a colorless powder.

^{1}H NMR (600 MHz, $CDCl_3$): δ 1.12–1.25 (m, 4H), 1.65–1.88 (m, 3H), 2.10–2.15 (m, 1H), 2.15–2.25 (m, 1H), 2.40–2.75 (m, 8H), 2.75–2.88 (4H, m), 3.32–3.42 (m, 1H), 3.88–4.05 (m, 1H), 7.17–7.23 (m, 3H), 7.28 (t, J = 7.6 Hz, 2H).

HRMS (DART) m/z calcd for $C_{17}H_{27}N_2O$ $(M+H)^+$, 289.2280; found 289.2284.

*2.1.7. trans-2-(4-(3-Phenylpropyl)piperazin-1-yl)cyclohexan-1-ol (**5**)*

Compound **2** (92 mg, 0.5 mmol) and 3-phenylpropyl bromide (100 mg, 0.5 mmol) were dissolved in 5 mL of acetonitrile and then potassium carbonate (69 mg, 0.5 mmol) was added to the solution. After reflux for 1 h, potassium carbonate was removed by filtration. The solvent was removed *in vacuo*. The residue was purified by chromatography on silica gel using chloroform-methanol (25:1) as the eluent to obtain compound **5** (61 mg, 41%) as a colorless powder.

^{1}H NMR (600 MHz, $CDCl_3$): δ 1.11–1.30 (m, 4H), 1.66–1.87 (m, 5H), 2.08–2.15 (m, 1H), 2.15–2.23 (m, 1H), 2.30–2.65 (m, 6H), 2.36 (t, J = 7.4 Hz, 2H), 2. (4H, m), 2.63 (t, J = 7.7 Hz, 2H), 2.72–2.82 (m, 2H), 3.32–3.40 (m, 1H), 3.90–4.06 (m, 1H), 7.16–7.22 (m, 3H), 7.28 (t, J = 7.6 Hz, 2H).

HRMS (DART) m/z calcd for $C_{19}H_{31}N_2O$ $(M+H)^+$, 303.2436; found 303.2403.

*2.1.8. trans-2-(4-(4-Phenylbutyl)piperazin-1-yl)cyclohexan-1-ol (**6**)*

Compound **2** (92 mg, 0.5 mmol) and 4-phenylbutyl bromide (106 mg, 0.5 mmol) were dissolved in 5 mL of acetonitrile and then potassium carbonate (69 mg, 0.5 mmol) was added to the solution. After reflux for 1 h, potassium carbonate was removed by filtration. The solvent was removed *in vacuo*. The residue was purified by chromatography on silica gel using chloroform-methanol (50:1) as the eluent to obtain compound **6** (61 mg, 39%) as a colorless powder.

^{1}H NMR (400 MHz, $CDCl_3$): δ 1.10–1.32 (m, 4H), 1.40–1.85 (m, 7H), 2.08–2.25 (m, 2H), 2.25–2.65 (m, 8H), 2.63 (t, J = 7.6 Hz, 2H), 2.68–2.83 (m, 2H), 3.30–3.40 (m, 1H), 3.90–4.10 (m, 1H), 7.15–7.20 (m, 3H), 7.27 (t, J = 7.9 Hz, 2H).

HRMS (DART) m/z calcd for $C_{20}H_{33}N_2O$ $(M+H)^+$, 317.2593; found 317.2621.

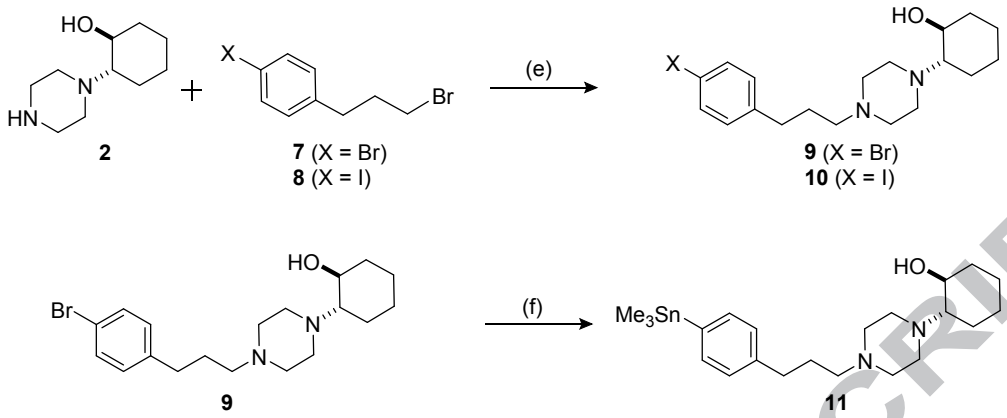

Scheme 2. Syntheses of compounds **9**–**11**.
(e) K_2CO_3, acetonitrile; (f) hexamethylditin,
tetrakis(triphenylphosphine)palladium(0), toluene.

2.1.9. trans-1-(3-Bromopropyl)-4-bromobenzene (7)

Triphenylphosphine (140 mg, 534 μmol) was dissolved in 1 mL of tetrahydrofuran (THF) at 0 ˚C, and then 3-(4-bromophenyl)propan-1-ol (100 mg, 465 μmol) and tetrabromomethane (180 mg, 543 mmol) in 1 mL of THF were added dropwise to the solution. After stirring for 4 h at room temperature under a nitrogen atmosphere, the solvent was removed *in vacuo*. The residue was purified by chromatography on silica gel using chloroform as the eluent to obtain compound **7** (82 mg, 64%) as yellow oil. ^{1}H NMR (400 MHz, $CDCl_3$): δ 2.14 (qt, J = 7.0 Hz, 2H), 2.74 (t, J = 7.3 Hz, 2H), 3.39 (t, J = 6.6 Hz, 2H), 7.08 (d, J = 8.2 Hz, 2H), 7.41 (d, J = 8.2 Hz, 2H).

*2.1.10. 1-(3-Bromopropyl)-4-iodobenzene (**8**)*

(3-Bromopropyl)benzene (100 mg, 0.5 mmol), iodine (50.7 mg, 0.2 mmol), and sodium iodate (20.8 mg, 0.1 mmol) were added to a mixture of 500 μL of acetic acid and 50 μL of concentrated sulfuric acid. After stirring for 18 h at 70 ˚C, the reaction solution was adjusted to pH 7-8 with saturated aqueous solution of sodium hydrogen carbonate, and was extracted with chloroform. The organic layer was dried with Na_2SO_4, and the solvent was removed *in vacuo*. The residue (**8**) was used in the next reaction without further purification.

*2.1.11. trans-2-(4-(3-(4-Bromophenyl)propyl)piperazin-1-yl)cyclohexan-1-ol (**9**)*

Compounds **2** (40 mg, 0.14 mmol) and **7** (27.6 mg, 0.15 mmol) were dissolved in 1.5 mL of acetonitrile and then potassium carbonate (20.7 mg, 0.15 mmol) was added to the solution. After reflux for 1 h, potassium carbonate was removed by filtration. The solvent was removed *in vacuo*. The residue was purified by chromatography on silica gel using

chloroform-methanol (40:1) as the eluent to obtain compound **9** (52 mg, 94%) as a colorless powder.

^{1}H NMR (400 MHz, $CDCl_3$): δ 1.10–1.32 (m, 4H), 1.65–1.85 (m, 5H), 2.07–2.25 (m, 2H), 2.35–2.55 (m, 6H), 2.34 (t, J = 7.6 Hz, 2H),2.58 (t, J = 7.6 Hz, 2H), 2.70–2.80 (m, 2H), 3.30–3.40 (m, 1H), 3.90–4.05 (m, 1H), 7.05 (d, J = 7.8 Hz, 2H), 7.39 (d, J = 7.8 Hz, 2H).

HRMS (DART) m/z calcd for $C_{19}H_{30}BrN_2O$ $(M+H)^+$, 381.1542; found 381.1548.

*2.1.12. trans-2-(4-(3-(4-Iodophenyl)propyl)piperazin-1-yl)cyclohexan-1-ol (**10**)*

Compounds **2** (5.7 mg, 30 μmol) and **8** (10 mg, 30 μmol) were dissolved in 300 μL of acetonitrile and then potassium carbonate (4.1 mg, 30 μmol) was added to the solution. After reflux for 1 h, potassium carbonate was removed by filtration. The solvent was removed *in vacuo*. The residue was purified by reversed phase (RP)-HPLC performed with a Cosmosil 5C_{18}-MS column (20 × 250 mm; Nacalai Tesque, Kyoto, Japan) at a flow rate of 12.0 mL/min with a gradient mobile phase of 80%

methanol in water with 0.05% triethylamine to 100% methanol with 0.05% triethylamine for 20 min. The fraction containing compound **10** was determined by mass spectrometry, and collected. The solvent was removed by lyophilization to yield compound **10** (4.0 mg, 17%) as a colorless powder.

^{1}H NMR (400 MHz, $CDCl_3$): δ 1.10–1.32 (m, 4H), 1.65–1.85 (m, 5H), 2.08–2.23 (m, 2H), 2.25–2.65 (m, 6H), 2.34 (t, J = 7.8 Hz, 2H), 2.57 (t, J = 7.6 Hz, 2H), 2.65–2.72 (m, 2H), 3.30–3.40 (m, 1H), 3.80–4.15 (m, 1H), 6.94 (d, J = 8.2 Hz, 2H), 7.59 (d, J = 8.2 Hz, 2H).

HRMS (DART) m/z calcd for $C_{19}H_{30}IN_2O$ $(M+H)^+$, 429.1403; found 429.1399.

*2.1.13. trans-2-(4-(3-(4-(Trimethylstannyl)phenyl)propyl)piperazin-1-yl)cyclohexan-1-ol (**11**)*

Compound **9** (38.1 mg, 0.10 mmol), hexamethylditin (81.9 mg, 0.25 mmol), and tetrakis(triphenylphosphine)palladium(0) (6.9 mg, 59.7 μmol) were dissolved in toluene. The reaction mixture was refluxed for 12 h under N_2 atmosphere. The solvent was removed *in vacuo*. The residue was

purified by chromatography on silica gel using chloroform as the eluent and RP-HPLC performed with a Cosmosil 5C_{18}-MS column (20 × 250 mm) at a flow rate of 12.0 mL/min with a gradient mobile phase of 75% methanol in water with 0.05% triethylamine to 85% methanol with 0.05% triethylamine for 20 min. The fraction containing compound **11** was determined by mass spectrometry, and collected. The solvent was removed by lyophilization to yield compound **11** (35 mg, 75%) as clear oil.

HRMS (ESI) m/z calcd for $C_{22}H_{39}N_2OSn$ $(M+H)^+$, 467.2084; found 467.2077.

2.2. In vitro competitive binding assay.

Samples of sigma-1 receptor and sigma-2 receptor for binding experiments were prepared from rat brains without cerebellum and rat liver in male Sprague-Dawley rats (200 g, Japan SLC, Inc., Hamamatsu, Japan) using a method described previously.[24, 25] A sigma-1 receptor binding assay and a sigma-2 receptor binding assay for compounds (+)-**1**, (–)-**1**, **3**-**6**, **10**, and reference compounds were performed by same methods described previously.[18]

*2.3. Preparation of [^{125}I]trans-2-(4-(3-(4-iodophenyl)propyl)piperazin-1-yl)cyclohexan-1-ol ([^{125}I]**10**)*

[^{125}I]**10** was prepared by a standard iodination reaction of the corresponding trimethylstannyl precursor. Briefly, 1 μL of [^{125}I]NaI solution was added to a reaction vial. Then, 100 μL of compound **11** (1 mg/mL in methanol), 15 μL of 10% acetic acid, and 20 μL of chroramine-T aqueous solution (4 mg/mL) were added to the reaction vial. After standing the reaction mixture at room temperature for 10 min, the reaction was quenched by adding of $NaHSO_3$ aqueous solution. The reaction mixture was purified by RP-HPLC performed using a Cosmosil 5C_{18}-MS-II column (4.6 × 150 mm; Nacalai Tesque) with a flow rate of 1 mL/min with a gradient mobile phase of 75% methanol in water with 0.05% triethylamine to 85% methanol in water with 0.05% triethylamine for 20 min. The column temperature was maintained at 40 °C.

2.4. Determination of partition coefficient

The partition coefficient of [^{125}I]**10** was measured as described

previously.[17] The partition coefficient was determined by calculating the ratio of radioactivity in 1-octanol to that in the 0.1 M phosphate buffer (pH 7.4), and expressed as a common logarithm (log *P*).

2.5. Cellular uptake experiments in vitro

Cellular uptake experiments were performed as described previously using a DU-145 prostate cancer cell lines (ATCC, Manassas, VA).[18] Briefly, the cells were seeded and pre-incubated on 6-well plates for 24 h, and incubated at 37 ºC in the culture medium without fetal bovine serum containing [^{125}I]**10** (3.7 kBq/well) or (+)-[^{125}I]*p*IV (3.7 kBq/well), which was prepared by a method of a previous report,[17] for different time intervals (15, 30, 60, and 120 min). The cell uptake of [^{125}I]**10** or (+)-[^{125}I]*p*IV was also examined by incubation with 10 μM of haloperidol as a blocking agent. After incubation, the cells were washed twice with ice-cold PBS and were resolved by 1 M NaOH. The solutions were then collected and the radioactivity was determined with an auto well gamma counter (ARC-7010; Hitachi Medical, Ltd., Tokyo, Japan) and corrected for background radiation. The radioactivity of each sample was normalized for

the protein level, which was determined using a Protein Assay Bicinchoninate Kit (Nacalai Tesque).

*2.6. Biodistribution experiments of [^{125}I]**10** in tumor-bearing mice*

The animal experimental protocols used were approved by the Committee on Animal Experimentation of Kanazawa University. Experiments with animals were conducted in accordance with the Guidelines for the Care and Use of Laboratory Animals of Kanazawa University. The animals were housed with free access to food and water at 23 ºC with a 12-h alternating light/dark schedule. Approximately 5×10^6 DU-145 cells were injected subcutaneously into the right dorsum of 4-week-old male BALB/c nude mice (15-19 g, Japan SLC, Inc.). After 14-21 days post-inoculation, mice were intravenously administered 100 μL of [^{125}I]**10** (37 kBq). At 1 and 24 h post-injection, the mice were sacrificed. Tissues of interest were removed and weighed, and radioactivity counts were determined with an auto well gamma counter.

2.7. Blocking studies in vivo

For blocking studies, the DU-145 tumor-bearing mice were intravenously administered 100 μL of [^{125}I] **10** (37 kBq) solution with an excess of an unlabeled sigma ligand, SA4503 (10 μmol/kg) or haloperidol (10 μmol/kg). At 1 h post-injection, the mice were sacrificed and biodistribution experiments were conducted as described above.

2.8. Statistical evaluation

All data were analyzed using GraphPad Prism 5.0 software (La Jolla, CA, USA) and displayed as mean ± standard deviation (SD). Significance for *in vitro* blocking studies was calculated using an unpaired Student's *t* test. Significance among three groups for *in vivo* blocking studies was calculated using a one-way analysis of variance (ANOVA) followed by Tukey's post hoc test. Results were considered statistically significant at $p < 0.05$.

3. Results and discussion

*3.1. Syntheses of compounds (+)-**1**, (–)-**1**, **3**–**6**, reference compound **10**, precursor **11**, and [^{125}I]**10***

The syntheses of compounds (+)-**1**, (–)-**1**, and **3**–**6** are outlined in Scheme 1. Compounds (+)-**1** and (–)-**1** were synthesized by a previously reported vesamicol synthesis method using phenylpiperazine as the starting material instead of phenylpiperidine.[26] Compounds **3**–**6** were synthesized using coupling compound **2** with phenyl alkyl bromide. However, the optical resolution of **3**–**6** by the same method as that applied for **1** was unsuccessful. Herein, an *in vitro* binding assay and other experiments were performed for the racemic compounds because these compounds are sufficient to achieve the purpose of this study, which is to evaluate the effect of the distance between the piperazine ring and the benzene ring.

The synthesis of the nonradioactive iodinated reference compound **10** and a labeling precursor **11** containing a trimethylstannyl group, which was prepared via brominated compound **9**, are outlined in Scheme 2. The overall yields of reference compound **10** and precursor **11** were 5% and 12%, respectively. Radioiodination of [^{125}I]**10** was performed by the standard electrophilic halogenation of the corresponding trimethylstannyl precursor **11** with a radiochemical yield of 75%. After purification by RP-HPLC, [^{125}I]**10** exhibited radiochemical purities exceeding 98%. The

identity of [^{125}I]**10** was confirmed by comparing its retention time with that of the corresponding nonradioactive iodinated reference compound **10** by HPLC (Figure 2).

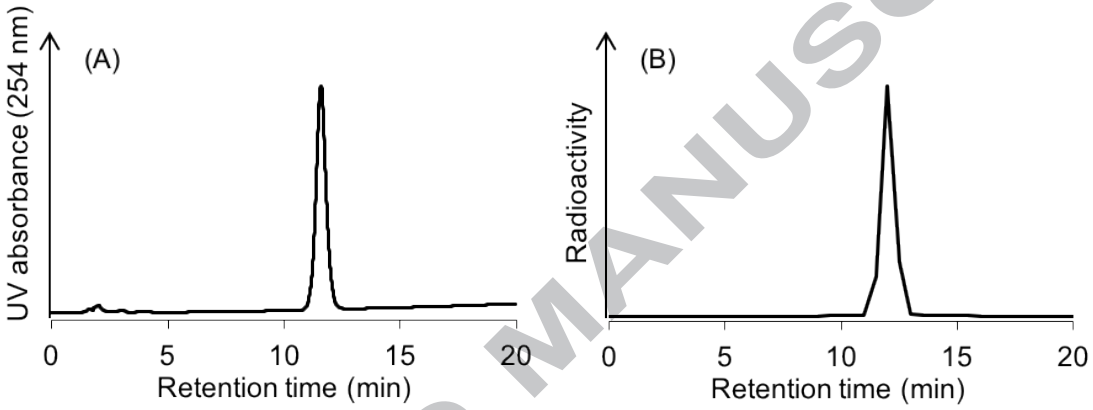

Figure 2. RP-HPLC chromatograms of (A) **10** and (B) [^{125}I]**10** after purification. Conditions: A flow rate of 1 mL/min with a gradient mobile phase of 75% methanol in water with 0.05% triethylamine to 85% methanol in water with 0.05% triethylamine for 20 min.

3.2. In vitro competitive binding assay

Table 1 lists the binding affinities of synthesized compounds (+)-**1**, (–)-**1**, **3**–**6**, **10**, and reference compounds for the sigma receptors (sigma-1 and sigma-2) determined by a competitive binding assay. The affinities of compounds **3** and **4** for sigma-1 receptor were similar and the affinities

were higher than those of compounds (+)-**1** and (–)-**1**. Furthermore, the affinities of compounds **5** and **6** for the sigma-1 receptor were similar and the affinities were higher than those of compounds **3** and **4**. Generally, the binding affinities for the sigma-1 and sigma-2 receptors of the aza-vesamicol homologs tended to increase as the length of the alkyl chain increased between the benzene ring and the piperazine ring. Compound **5** showed the lowest *K*i value (*K*i = 5.8 nM) among compounds (+)-**1**, (–)-**1**, and **3** – **6** and the affinity of compound **5** for the sigma-1 receptor was higher than those of the reference compounds utilized as selective and non-selective sigma-1 receptor ligands: (+)-pentazocine (*K*i = 16.0 nM) and haloperidol (*K*i = 12.5 nM), respectively. Therefore, we introduced iodine or radioiodine into the benzene ring in compound **5**. The *para* position of the phenyl group was selected as the introduction site because *p*IV (Figure 1b), a vesamicol analog with an iodine at the *para* position, had the highest affinity for the sigma-1 receptor among vesamicol analogs in which iodine was introduced at different positions of the phenyl group in our previous studies [(+)-vesamicol: *K*i = 74.9 nM, (+)-*p*IV: *K*i = 1.3 nM].[16, 24] We expected the affinity for the sigma-1 receptor to increase because of the

increased affinity resulting from the introduction of iodine into the benzene ring in the case of vesamicol;[16, 17] however, upon the introduction of iodine to **5**, the affinity for the sigma-1 receptor showed little change. This unexpected result may be attributed to the large distance between the benzene ring and piperazine ring. These results indicate that the optimal halogen introduction position might not necessarily be the *para* position in aza-vesamicol compounds.

Meanwhile, compound **10** showed low selectivity for the sigma-1 receptor against the sigma-2 receptor (*K*i for sigma-1 = 8.7 nM and *K*i for sigma-2 = 22.3 nM, respectively). For receptor imaging in the brain, selectivity is important. However, sigma-1 and sigma-2 dual receptor imaging probes have also been studied, and their usefulness has been evaluated for prostate cancer imaging.[27] Thus, the affinity of compound **10** for the sigma receptors may be suitable for prostate cancer imaging.

Table 1. Affinities (nM) of synthesized vesamicol derivatives and reference compounds for sigma receptors.

	Sigma-1 (K_i)	Sigma-2 (K_i)
(+)-**1**	85.3 ± 20.2	328.0 ± 26.9
(–)-**1**	87.3 ± 9.0	245.6 ± 45.3
3	33.2 ± 7.7	723.0 ± 67.7
4	31.5 ± 4.2	246.2 ± 69.9
5	5.8 ± 0.9	50.4 ± 13.0
6	9.0 ± 1.7	31.2 ± 4.9
10	8.7 ± 1.0	22.3 ± 3.5
(+)-Pentazocine	16.0 ± 1.6	2437.2 ± 313.4
Haloperidol	12.5 ± 0.9	81.5 ± 38.5

K_i values derived from IC_{50} values according to the equation: $K_i = IC_{50}/(1 + C/K_d)$, where C is the concentration of the radioligand and each K_d is the dissociation constant of the corresponding radioligand ([^{3}H]pentazocine to sigma-1 (K_d = 19.9 nM), [^{3}H]DTG to sigma-2 (K_d = 22.3 nM)).
Values are means ± SEM of three experiments.

3.3. Partition coefficient

The partition coefficient was determined, and the log *P* value of [^{125}I]**10** was found to be 2.54 ± 0.04 (mean ± SD for four samples). This result indicates that the lipophilicity of [^{125}I]**10** is higher than that of (+)-[^{125}I]*p*IV, whose log *P* value is 2.08.[17] The higher lipophilicity of [^{125}I]**10** is

attributed to from the alkyl chain of **10** between the benzene ring and the piperazine ring.

3.4. In vitro cellular uptake experiments

Cellular uptake experiments of [^{125}I]**10** into DU145 cells demonstrated a rapid and substantial uptake (Figure 3B), and its uptake was higher than that of [^{125}I]*p*IV (Figure 3A). The uptake of [^{125}I]**10** was considerably inhibited in the presence of an excess amount of haloperidol (10 μM in the culture medium), which is a sigma-1 receptor ligand. However, the degree of inhibition of [^{125}I]**10** by haloperidol was lower than that of [^{125}I]*p*IV. Nonspecific binding or uptake of [^{125}I]**10** into DU145 cells may have occurred because of its relatively high lipophilicity. Previous studies have also suggested that sigma-1 receptor ligands with suitable lipophilicity for tumor imaging may be useful for reducing nonspecific accumulation.[28, 29]

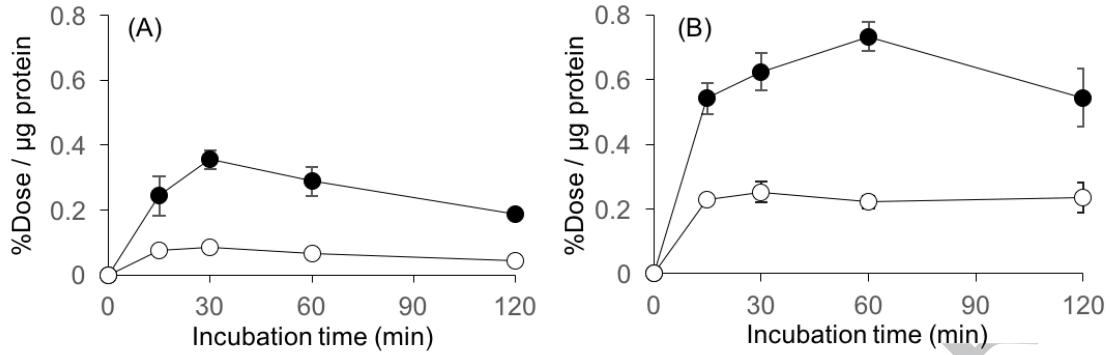

Figure 3. Cellular uptake experiments. Time-dependent accumulation of [^{125}I]*p*IV (A) and [^{125}I]**10** (B) in DU145 tumor cells with (open circle) or without (closed circle) the addition of haloperidol (10 µM) into the culture medium. Data are expressed as mean ± SD for three samples.

*3.5. In vivo biodistribution experiments of [^{125}I]**10** in tumor-bearing mice and blocking studies.*

Table 2 demonstrates the biodistribution of [^{125}I]**10** in DU145 tumor-bearing mice. [^{125}I]**10** exhibited a high accumulation and long retention in tumor. [^{125}I]**10** also showed a high accumulation in nonspecific tissues such as the liver, kidney, and lung, at 1 h post-injection. The biodistribution pattern of [^{125}I]**10** was similar to that of (+)-[^{125}I]*p*IV. At 24 h post-injection, [^{125}I]**10** showed a more favorable biodistribution, i.e., similar tumor uptake and lower accumulation in most non-target tissues than (+)-[^{125}I]*p*IV. Therefore, the tumor/blood ratio and tumor/muscle ratio

of [^{125}I]**10** (31.6 and 24.4, respectively) were higher than those of (+)-[^{125}I]*p*IV (12.4 and 14.3, respectively) at 24 h post-injection.

Table 3 presents the tumor uptake at 1 h post-injection for (+)-[^{125}I]**10** with and without an excess amount of a sigma receptor ligand, SA4503 or haloperidol, in tumor-bearing mice. The %dose/gram value was significantly decreased by co-injection of an excess amount of SA4503 or haloperidol. However, the inhibition by sigma receptor ligands was lower than expected; the inhibition was found to be significant but not sufficient in an *in vitro* cell uptake study. The cell uptake study indicated that possibility of nonspecific accumulation in tumor may be derived from high lipophilicity of [^{125}I]**10**. Meanwhile, the moderate affinity of [^{125}I]**10** for the sigma-2 receptor (*K*i = 22.3 nM) may also contribute to the tumor accumulation of [^{125}I]**10**. A previous study reported that both (+)-[^{3}H]pentazocine and [^{3}H]DTG in the presence of dextrallorphan showed high-affinity binding in DU-145,[30] indicating thathe sigma-1 receptor but also the sigma-2 receptor is overexpressed in DU-145. However, the biodistributions of [^{125}I]**10** in the *in vivo* blocking study using SA4503 (a selective sigma-1 receptor ligand) or haloperidol (a non-selective sigma

receptor ligand) were similar, as no statistically significant differences were observed between the %dose/gram values in any tissues for the SA4503-treated group and the haloperidol-treated group (Table 3). Therefore, the *in vivo* blocking study results indicate that the sigma-2 receptor may have little effect on the biodistribution of [^{125}I]**10**.

4. Summary

Herein, several aza-vesamicol homologs were synthesized and their affinities for sigma receptors were evaluated. Generally, the affinities for sigma receptors tended to increase with increasing length between the piperidine ring and the benzene ring. Since compound **5** exhibited the lowest *K*i value for the sigma-1 receptor, iodine or radioiodine was introduced into the benzene ring in compound **5,** and the resultant compounds **10** or [^{125}I]**10** were evaluated. [^{125}I]**10** with a high affinity for the sigma-1 receptor was prepared with high radiochemical yields and high radiochemical purities. Compared with (+)-[^{125}I]*p*IV, [^{125}I]**10** showed a better biodistribution as a sigma-1 imaging probe at 24 h post-injection.

These results provide useful information for the development of sigma-1 receptor imaging probes.

Table 2. Biodistribution of radioactivity after intravenous injection of [^{125}I]**10** or (+)-[^{125}I]*p*IV in DU145 tumor-bearing mice.

Tissue	[^{125}I]**10**		
	Time after injection		
	1 h	24 h	48 h
Blood	0.78 (0.09)	0.20 (0.03)	0.13 (0.01)
Tumor	6.23 (0.55)	6.27 (2.36)	2.54 (0.59)
Liver	26.02 (1.99)	7.42 (0.48)	4.89 (0.18)
Kidney	26.15 (2.08)	3.41 (0.58)	2.27 (0.40)
Small Intestine	12.19 (0.70)	3.00 (0.63)	2.30 (0.19)
Large Intestine	4.11 (0.38)	2.02 (0.31)	3.06 (0.40)
Spleen	14.87 (0.99)	2.15 (0.31)	1.37 (0.31)
Lung	18.00 (3.18)	1.89 (0.51)	0.88 (0.12)
Heart	3.66 (0.32)	0.40 (0.08)	0.23 (0.04)
Stomach†	1.73 (0.41)	0.52 (0.33)	0.26 (0.20)
Brain	4.77 (0.60)	0.66 (0.13)	0.30 (0.01)
Muscle	1.84 (0.36)	0.26 (0.09)	0.13 (0.03)
T/B ratio‡	8.06 (0.89)	31.56 (9.46)	19.57 (3.44)
T/M ratio§	3.48 (0.57)	24.35 (7.27)	20.59 (4.79)
Tissue	(+)-[^{125}I]*p*IV*		
	Time after injection		
	1 h	24 h	48 h
Blood	0.24 (0.03)	0.71 (0.05)	0.37 (0.06)
Tumor	6.27 (1.00)	8.78 (0.41)	6.04 (1.19)

Liver	16.91 (0.79)	15.23 (0.62)	5.24 (0.41)
Kidney	16.24 (2.52)	9.38 (0.60)	4.21 (0.28)
Intestine	6.44 (1.10)	4.89 (0.16)	1.50 (0.19)
Spleen	13.62 (2.73)	4.04 (0.53)	1.75 (0.25)
Lung	15.62 (5.87)	3.83 (0.44)	1.81 (0.62)
Heart	8.21 (1.85)	1.62 (0.21)	0.65 (0.07)
Stomach†	0.66 (0.09)	0.59 (0.05)	0.27 (0.05)
Brain	7.65 (2.15)	2.89 (0.10)	1.08 (0.09)
Muscle	2.41 (0.77)	0.64 (0.17)	0.30 (0.09)
T/B ratio‡	26.20 (4.23)	12.39 (0.98)	16.48 (2.16)
T/M ratio§	2.72 (0.55)	14.30 (2.76)	20.54 (2.02)

Data are expressed as % injected dose per gram tissue. Each value represents the mean (SD) for from three to five animals.

*Biodistribution data of (+)-[^{125}I]*p*IV from reference.[17]

†Data are expressed as % injected dose.

‡Tumor:blood ratio.

§Tumor:muscle ratio.

Table 3. Comparison of biodistribution of [^{125}I]**10** at 1 h post-injection under no-carrier-added condition (control) and under co-injection of SA4503 or haloperidol.

Tissue	[^{125}I]**10** at 1 h (blocking)		
	Control	SA4503	Haloperidol
Blood	0.78 (0.09)	0.59 (0.01)	0.69 (0.31)
Tumor	6.23 (0.55)	4.06 (0.15)***	3.60 (0.49)***
Liver	26.02 (1.99)	15.09 (1.28)***	13.10 (2.24)***
Kidney	26.15 (2.08)	9.17 (0.51)***	12.20 (2.77)***
Small Intestine	12.19 (0.70)	10.66 (2.18)	11.27 (4.17)
Large Intestine	4.11 (0.38)	2.97 (0.05)**	3.31 (0.38)*
Spleen	14.87 (0.99)	9.04 (1.07)	14.94 (5.93)
Lung	18.00 (3.18)	7.54 (1.73)**	10.00 (4.13)*
Heart	3.66 (0.32)	1.91 (0.09)**	2.99 (1.01)
Stomach†	1.73 (0.41)	1.74 (0.72)	2.13 (1.09)
Brain	4.77 (0.60)	3.74 (0.22)	4.79 (0.76)
Muscle	1.84 (0.36)	0.93 (0.06)*	1.66 (0.58)
T/B ratio‡	8.06 (0.89)	6.88 (0.44)	5.85 (1.61)*
T/M ratio§	3.48 (0.57)	4.36 (0.19)*,#	2.32 (0.41)**

Data are expressed as % injected dose per gram tissue. Each value represents the mean (SD) for four animals.

†Data are expressed as % injected dose.

‡Tumor:blood ratio.

[§]Tumor:muscle ratio.

Significance was determined using one-way ANOVA followed by Tukey's post hoc test (*$p < 0.05$, **$p < 0.01$, and ***$p < 0.001$ vs. control), ([#]$p < 0.001$ vs. Haloperidol).

Acknowledgments

This work was supported in part by Takeda Science Foundation, Kato Memorial Bioscience Foundation, Hokkoku Foundation for Cancer Research, and the Matsubara Saburo Memorial Research and Scholarship Fund.

Conflict of interest

The authors have declared that no conflict of interest.

References

1. Martin WR, Eades CG, Thompson JA, Huppler RE, Gilbert PE. The effects of morphine- and nalorphine- like drugs in the nondependent and morphine-dependent chronic spinal dog. *J Pharmacol Exp Ther*. 1976;197:517-532.

2. Quirion R, Bowen WD, Itzhak Y, Junien JL, Musacchio JM, Rothman RB, Su TP, Tam SW, Taylor DP. A proposal for the classification

of sigma binding sites. *Trends Pharmacol Sci*. 1992;13:85-86.

3. Hanner M, Moebius FF, Flandorfer A, Knaus HG, Striessnig J, Kempner E, Glossmann H. Purification, molecular cloning, and expression of the mammalian sigma1-binding site. *Proc Natl Acad Sci U S A*. 1996;93:8072-8077.

4. Alon A, Schmidt HR, Wood MD, Sahn JJ, Martin SF, Kruse AC. Identification of the gene that codes for the sigma2 receptor. *Proc Natl Acad Sci U S A*. 2017;114:7160-7165.

5. Hayashi T, Tsai SY, Mori T, Fujimoto M, Su TP. Targeting ligand-operated chaperone sigma-1 receptors in the treatment of neuropsychiatric disorders. *Expert Opin Ther Targets*. 2011;15:557-577.

6. Ogawa K, Masuda R, Shiba K. Development of Radiolabeled Probes Directed against Sigma-1 Receptors. *BUNSEKI KAGAKU*. 2017;66:403-411.

7. Miki Y, Mori F, Kon T, Tanji K, Toyoshima Y, Yoshida M, Sasaki H, Kakita A, Takahashi H, Wakabayashi K. Accumulation of the sigma-1 receptor is common to neuronal nuclear inclusions in various neurodegenerative diseases. *Neuropathology*. 2014;34:148-158.

8. Mavlyutov TA, Epstein ML, Verbny YI, Huerta MS, Zaitoun I, Ziskind-Conhaim L, Ruoho AE. Lack of sigma-1 receptor exacerbates ALS progression in mice. *Neuroscience*. 2013;240:129-134.

9. Weng TY, Tsai SA, Su TP. Roles of sigma-1 receptors on mitochondrial functions relevant to neurodegenerative diseases. *J Biomed Sci*. 2017;24:74.

10. Vilner BJ, John CS, Bowen WD. Sigma-1 and sigma-2 receptors are expressed in a wide variety of human and rodent tumor cell lines. *Cancer Res*. 1995;55:408-413.

11. Crottes D, Guizouarn H, Martin P, Borgese F, Soriani O. The sigma-1 receptor: a regulator of cancer cell electrical plasticity? *Front Physiol*. 2013;4:175.

12. Yang S, Bhardwaj A, Cheng J, Alkayed NJ, Hurn PD, Kirsch JR. Sigma receptor agonists provide neuroprotection in vitro by preserving bcl-2. *Anesth Analg*. 2007;104:1179-1184, tables of contents.

13. Happy M, Dejoie J, Zajac CK, Cortez B, Chakraborty K, Aderemi J, Sauane M. Sigma 1 Receptor antagonist potentiates the anti-cancer effect of p53 by regulating ER stress, ROS production, Bax levels, and caspase-3

activation. *Biochem Biophys Res Commun*. 2015;456:683-688.

14. Collier TL, Waterhouse RN, Kassiou M. Imaging sigma receptors: applications in drug development. *Curr Pharm Des*. 2007;13:51-72.

15. van Waarde A, Rybczynska AA, Ramakrishnan NK, Ishiwata K, Elsinga PH, Dierckx RA. Potential applications for sigma receptor ligands in cancer diagnosis and therapy. *Biochim Biophys Acta*. 2015;1848:2703-2714.

16. Shiba K, Ogawa K, Mori H. In vitro characterization of radioiodinated (+)-2-[4-(4-iodophenyl) piperidino]cyclohexanol [(+)-pIV] as a sigma-1 receptor ligand. *Bioorg Med Chem*. 2005;13:1095-1099.

17. Ogawa K, Shiba K, Akhter N, Yoshimoto M, Washiyama K, Kinuya S, Kawai K, Mori H. Evaluation of radioiodinated vesamicol analogs for sigma receptor imaging in tumor and radionuclide receptor therapy. *Cancer Sci*. 2009;100:2188-2192.

18. Ogawa K, Kanbara H, Shiba K, Kitamura Y, Kozaka T, Kiwada T, Odani A. Development and evaluation of a novel radioiodinated vesamicol analog as a sigma receptor imaging agent. *EJNMMI Res*. 2012;2:54.

19. Ogawa K, Kanbara H, Kiyono Y, Kitamura Y, Kiwada T, Kozaka

T, Kitamura M, Mori T, Shiba K, Odani A. Development and evaluation of a radiobromine-labeled sigma ligand for tumor imaging. *Nucl Med Biol*. 2013;40:445-450.

20. Ogawa K, Mizuno Y, Washiyama K, Shiba K, Takahashi N, Kozaka T, Watanabe S, Shinohara A, Odani A. Preparation and evaluation of an astatine-211-labeled sigma receptor ligand for alpha radionuclide therapy. *Nucl Med Biol*. 2015;42:875-879.

21. Ogawa K, Masuda R, Mizuno Y, Makino A, Kozaka T, Kitamura Y, Kiyono Y, Shiba K, Odani A. Development of a novel radiobromine-labeled sigma-1 receptor imaging probe. *Nucl Med Biol*. 2018;61:28-35.

22. Georgiadis MO, Karoutzou O, Foscolos AS, Papanastasiou I. Sigma Receptor (sigmaR) Ligands with Antiproliferative and Anticancer Activity. *Molecules*. 2017;22.

23. Schmidt HR, Zheng S, Gurpinar E, Koehl A, Manglik A, Kruse AC. Crystal structure of the human sigma1 receptor. *Nature*. 2016;532:527-530.

24. Shiba K, Yano T, Sato W, Mori H, Tonami N. Characterization of radioiodinated (-)-ortho-iodovesamicol binding in rat brain preparations.

Life Sci. 2002;71:1591-1598.

25. Shiba K, Mori H, Matsuda H, Tsuji S, Kuji I, Sumiya H, Kinuya K, Tonami N, Hisada K, Sumiyosi T. Synthesis of radioiodinated analogs of 2-(4-phenylpiperidino)cyclohexanol (vesamicol) as vesamicol-like agent. *Nucl Med Biol*. 1995;22:205-210.

26. Rogers GA, Parsons SM, Anderson DC, Nilsson LM, Bahr BA, Kornreich WD, Kaufman R, Jacobs RS, Kirtman B. Synthesis, in vitro acetylcholine-storage-blocking activities, and biological properties of derivatives and analogues of trans-2-(4-phenylpiperidino)cyclohexanol (vesamicol). *J Med Chem*. 1989;32:1217-1230.

27. Yang D, Comeau A, Bowen WD, Mach RH, Ross BD, Hong H, Van Dort ME. Design and Investigation of a [^{18}F]-Labeled Benzamide Derivative as a High Affinity Dual Sigma Receptor Subtype Radioligand for Prostate Tumor Imaging. *Mol Pharm*. 2017;14:770-780.

28. Xie F, Bergmann R, Kniess T, Deuther-Conrad W, Mamat C, Neuber C, Liu B, Steinbach J, Brust P, Pietzsch J, Jia H. ^{18}F-Labeled 1,4-Dioxa-8-azaspiro[4.5]decane Derivative: Synthesis and Biological Evaluation of a sigma1 Receptor Radioligand with Low Lipophilicity as

Potent Tumor Imaging Agent. *J Med Chem*. 2015;58:5395-5407.

29. Wang X, Li D, Deuther-Conrad W, Lu J, Xie Y, Jia B, Cui M, Steinbach J, Brust P, Liu B, Jia H. Novel cyclopentadienyl tricarbonyl ^{99m}Tc complexes containing 1-piperonylpiperazine moiety: potential imaging probes for sigma-1 receptors. *J Med Chem*. 2014;57:7113-7125.

30. John CS, Vilner BJ, Geyer BC, Moody T, Bowen WD. Targeting sigma receptor-binding benzamides as in vivo diagnostic and therapeutic agents for human prostate tumors. *Cancer Res*. 1999;59:4578-4583.

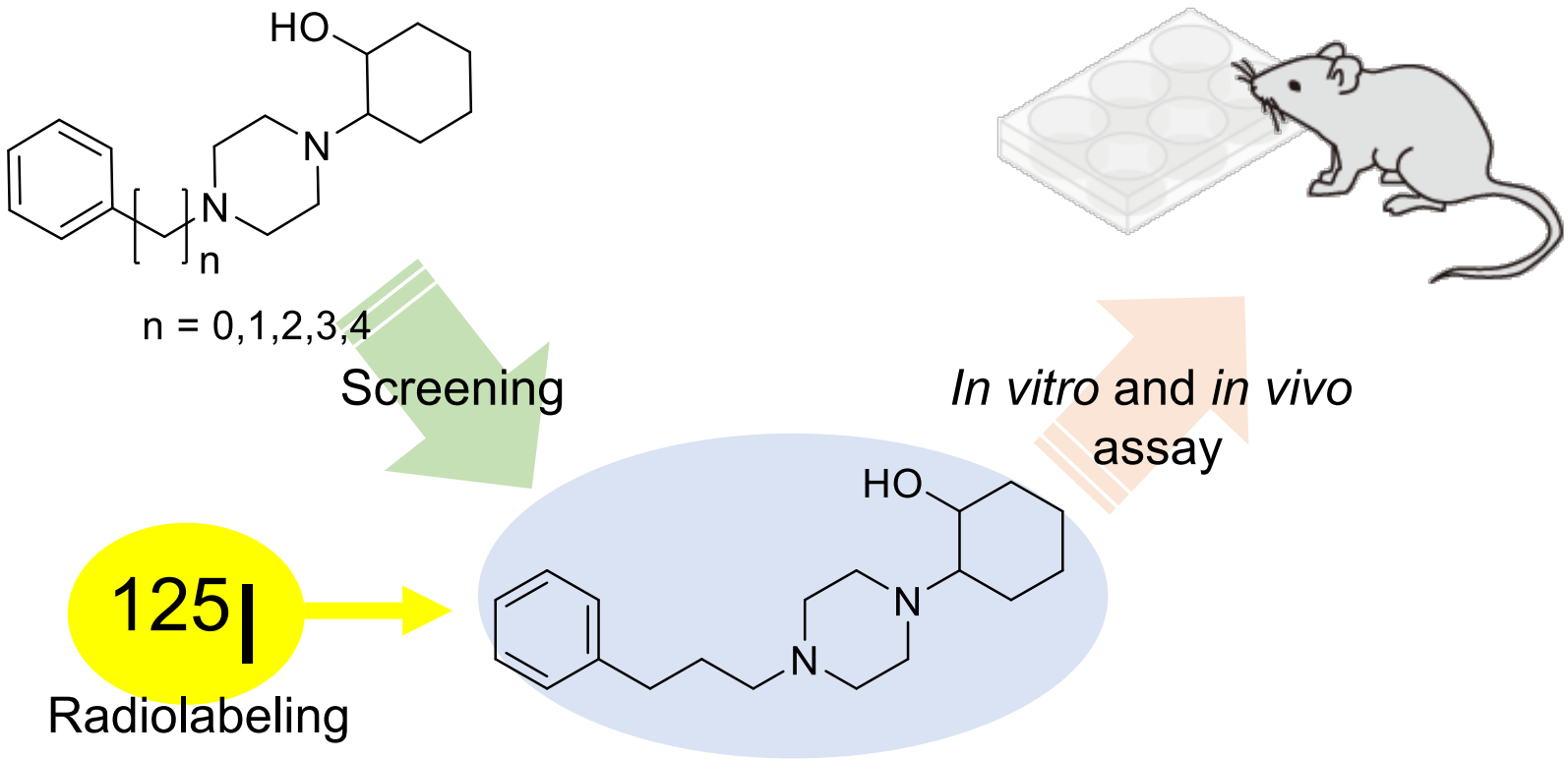
HO
N
N
n
n = 0,1,2,3,4
Screening
In vitro and in vivo
assay
125I
Radiolabeling
HO
N
N